Status of a UAV SAR Designed for Repeat Pass Interferometry for Deformation Measurements

Scott Hensley, Kevin Wheeler, Jim Hoffman, Tim Miller, Yunling Lou, Ron Muellerschoen, Howard Zebker[†], Søren Madsen and Paul Rosen

Jet Propulsion Laboratory
California Institute of Technology
4800 Oak Grove Drive
Pasadena, California 91109

[†]Stanford University
MC 9515
334 Packard Electrical Engineering
Palo Alto, California, 94305

Abstract - **Under the NASA ESTO sponsored Instrument Incubator Program we have designed a light-weight, reconfigurable polarimetric L-band SAR designed for repeat pass deformation measurements of rapidly deforming surfaces of geophysical interest such as volcanoes or earthquakes. This radar will be installed on an unmanned airborne vehicle (UAV) or a lightweight, high-altitude, and long endurance platform such as the Proteus. After a study of suitable available platforms we selected the Proteus for initial development and testing of the system. We want to control the repeat track capability of the aircraft to be within a 10 m tube to support the repeat deformation capability. We conducted tests with the Proteus using real-time GPS with sub-meter accuracy to see if pilots could fly the aircraft within the desired tube. Our results show that pilots are unable to fly the aircraft with the desired accuracy and therefore an augmented autopilot will be required to meet these objectives. Based on the Proteus flying altitude of 13.7 km (45,000 ft), we are designing a fully polarimetric L-band radar with 80 MHz bandwidth and 16 km range swath. This radar will have an active electronic beam steering antenna to achieve Doppler centroid stability that is necessary for repeat-pass interferometry. This paper will present are design criteria, current design and expected science applications.**

I. INTRODUCTION

The solid earth science community is seeking earth deformation measurements at a variety of scales, from seconds to decades. The NASA Solid Earth Science Working Group has recommended an observational program that includes both airborne and spaceborne capabilities and this is reflected in the NASA Earth Science Enterprise strategic plan[‡]. Ultimately, scientists would like to have earth deformation measurements on an hourly basis with global access, objectives best supported by a spaceborne high-orbit (e.g. geosynchronous) constellation of repeat-pass interferometric SAR satellites. The recommended first step in this observational program is a low-earth-orbit deformation satellite with a repeat period of roughly one week. The sub-orbital radar program enters the Earth Science Enterprise plan as a key supplemental capability, providing repeat-pass measurements at time scales much smaller than one week, potentially as short as twenty minutes.

Understanding the time varying nature of rapidly deforming features such as some volcanoes and glaciers or deformation from post seismic transients requires observational sampling intervals of a day or less to capture and model such events. In addition to providing unprecedented temporal detail of deformation of dynamic processes, the suborbital radar will be a testbed for understanding the observational needs for how rapid repeat observations would be acquired. This is a capability that the currently operational NASA AIRSAR system has demonstrated but cannot practically support for science experiments in its current configuration due to lack of track repeatability and beam pointing limitations.

A proposal was submitted to the NASA 2002 Instrument Incubator Program (IIP) to develop a repeat pass measurement capability as an augmentation to the existing AIRSAR system. NASA accepted the proposal but directed that the proposed capability be fielded on a UAV or MPV platform to support the long term interests of the airborne science community and that the first year effort be devoted to developing a radar system design and implementation plan. This paper presents the results of the first year of study and the resulting radar design.

II. PLATFORM SELECTION

Reliable collection and processing of airborne repeat pass radar interferometric data for deformation measurements imposes additional platform and radar instrument constraints on a UAV platform not normally required by standard SAR

[‡] http://www.earth.nasa.gov/visions/stratplan/index.html

imaging systems. The platform needs to fly within a 10 m diameter tube (with a 1 m goal). This provides a small repeat-pass baseline desired for deformation measurements as well as an ability to fly the same path multiple times with multiple time scales for reliable acquisition of the desired science data. Flying trajectories this accurately requires real-time platform position knowledge with sub-meter accuracy. Such position accuracy is possible based on previously developed real-time GPS platform position determination capability (20-50 cm) that then must be interfaced with the platform flight management system (FMS). The radar modifications required to support repeat-pass deformation measurements include:

- Radar should support electronic steering of antenna beam with 1° accuracy over a range of ±15° in azimuth so that the repeat pass pointing requirements can be achieved for a wide variety of wind conditions aloft.
- Electronic steering of antenna must be linked to the inertial navigation unit (INU) attitude measurements with an update rate capability of less than one second.
- L-band is required to maintain interferometric coherence over large repeat time observation intervals and coupled with maximal allowed bandwidth of 80 MHz have the largest possible critical baseline.

Figure 2 illustrates the desired flight track and radar electronic pointing capability desired for airborne repeat pass observations.

One of the main tasks for fielding the new system is selection of a platform from the currently operational UAV or minimally piloted vehicles (MPV) that meet the following requirements.

- Operate in a variety of weather conditions
- Operate from conventional airports
- Operate above 12,000 meters to avoid commercial traffic and reduce turbulence
- Maintain a flight path with positional accuracy of ±5 meters
- Has a minimum range of 2000 nautical miles
- Has a minimum payload capacity of 300 kilograms
- Has a minimum payload volume of 1 cubic meter
- Has a minimum 2,000 watts of DC power available for the payload
- Support over-the-horizon up/downlink
- Able to mount an external, side-looking, active array antenna (0.5m by 2.0m) without obstruction

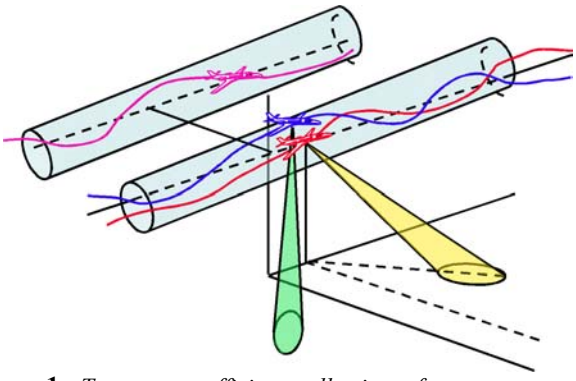

Figure 1. *To support efficient collection of repeat pass radar interferometry data the platform must be able to fly the same trajectory within a specified tube illustrated above in the tube with the red and blue aircraft. Since the yaw or crab angle of the aircraft can change between repeat pass lines the radar will use an electronically scanned antenna to compensate for the different aircraft yaw angles between passes. Additional science such as very high resolution topographic mapping or tomograhic imaging studies may also be supported by flying well defined baselines illustrated by the magenta aircraft flying on a trajectory displaced by a fixed amount from some reference trajectory.*

Studies conducted during the past year identified the Proteus and Altair platforms as the best candidates to host the UAVSAR. A brief summary of these platforms and a study we conducted with the Proteus aircraft to assess the ability of a pilot to fly within a 10 m tube are described below.

A. Survey of UAV Capabilities

Table 1 gives the operating parameters for the two candidate platforms suitable for hosting the UAVSAR L-band radar. Both platforms met the criteria specified for the platform including loiter altitude, the true air speed, the range, and the payload weight. Also, very importantly both platforms have excess power, mass and volume to meet future needs for upgrading and extending the capabilities of the UAVSAR.

NASA's Environmental Research Aircraft and Sensor Technology (ERAST) program has conducted some flight tests with both the Proteus UAV and the Predator-B UAV. Between the two UAVs, the Proteus is the larger and more capable platform. However, the Proteus currently requires a two-person crew for landing and takeoff. In addition, there is only one Proteus aircraft available for scientific experiments. Experiments are conducted on a first-come first-serve basis. NASA or other government agencies fund most of the payloads. The availability of the aircraft for radar experiments will probably be limited. On the other hand, NASA signed a contract with General Atomics in early 2000 for the development of two enhanced Predator-B UAVs (ALTAIR) to perform high altitude Earth science missions.

Flight tests for the ALTAIR UAV began in Spring 2003. The ALTAIR is based on General Atomics Aeronautical Systems, Inc.'s (GA-ASI) family of UAVs with over 35,000 flight hours in deployments for scientific, military, and civil applications. Hence, the availability and reliability of the ALTAIR is likely to be higher than the Proteus aircraft.

Table 1. Platform Candidates

Plat-form	Alt (m)	Spd (kts)	L (m)	Wings (m)	Rng (nmi)	Pay-load weight (kg)
ALTAIR	13,700	220	8.23	14.84	32 hrs	340
Proteus	19,800	450	17.2	23.6	9,000 24 hrs	900
DC-8	12000	400	47.8	45.1	5400 12 □ □□	∞

In light of the NASA requirement to replace the NASA DC-8 and ER-2s with UAVs and the Proteus aircraft to support Earth Science missions, we need to design a radar system that is capable of data acquisition on both the ALTAIR UAV and the Proteus aircraft with minimal modifications.

ALTAIR UAV: Enhanced Predator-B produced by General Atomics Aeronautical Systems, Inc. for NASA

Proteus Aircraft: Operated by Scaled Composites in Mojave. One-of-a-kind platform

Figure 2. *Two aircraft platforms are currently being considered to host the UAVSAR radar. Altair is a UAVs while Proteus is a MPV.*

We have selected the Proteus as the initial platform for installation of the UAVSAR radar. Selection was based on the easier access to the National Airspace (NAS) for an MPV platform such as Proteus, having a pilot onboard to help with instrument checkout early in the flight test program, and the greater ability of the platform to support future modes such a along track interferometry.

B. Origin of the 10 Tube Requirement

An important aspect of repeat pass interferometry is the ability to control the flight track. Two physical mechanisms drive the repeat pass baseline to be less 10 m. The two primary observables of a radar interferometer are the phase and interferometric correlation. The interferometric phase encodes the deformation signal of geophysical interest. The interferometric correlation, γ, measures the similarity of the signal received by the two antennas forming the interferometric pair. A maximal value of 1 is obtained when the signals are perfectly correlated and a value of 0 is obtained when the signals are completely uncorrelated. The interferometric correlation can be written as

$$\gamma = \gamma_g \gamma_{snr} \gamma_{vol} \gamma_{rot} \gamma_t \tag{1}$$

where γ_g is the geometric correlation that is function of physical separation between the antennas, γ_{snr} which is the correlation due to thermal noise, γ_{vol} is the volumetric correlation which is sensitive to the vertical structure within a resolution element, γ_{rot} is the rotational correlation which is sensitive to the relative rotation of the of scatterers within a resolution element and γ_t is the temporal correlation which is sensitive to wavelength scale changes within a resolution element. For deformation mapping we require correlation levels above a certain threshold. The geometric correlation decreases as the baseline length increases and thus it is necessary to make sure the baseline is not too long.

For deformation mapping applications generally the geometric correlation levels should be above 0.8 to allow for decreased correlation resulting from changes within a resolution element between observations, i.e. temporal decorrelation. An expression for the geometric correlation is given by

$$\gamma_g = 1 - \frac{2p}{\lambda} \frac{b\cos(\theta - \alpha)}{\rho \tan(\theta - \tau_{xt})} \Delta\rho = 1 - \frac{2p}{\lambda} \frac{b\cos(\theta)\cos(\theta - \alpha)}{h_p \tan(\theta - \tau_{xt})} \Delta\rho \tag{2}$$

where θ is the look angle, b is the baseline length, α is the baseline orientation angle of the baseline vector with respect to the local horizontal, λ is the wavelength, h_p is the height of the platform, τ_{xt} is the slope of the terrain in the cross track direction and $\Delta\rho$ is the range resolution which is a function of the transmitted range bandwidth. Figure 3 shows the geometric correlation for a platform height of 14000 m and an incidence angle of 45° for several values of the cross track surface slope. To have correlation values of .8 for surface slopes up to 40° requires that the baseline length be less than 25 m.

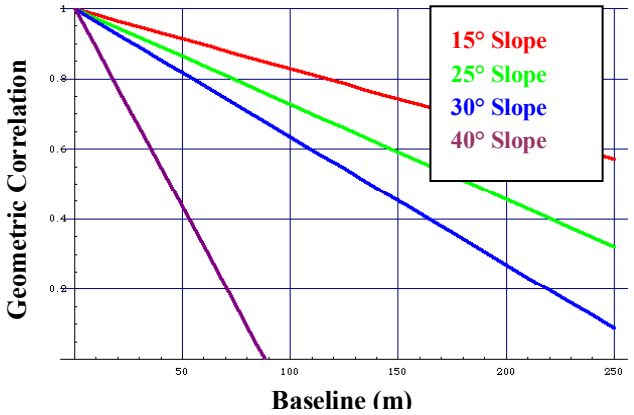

Figure 3. *Plots of the geometric correlation as a function of baseline length for cross track slopes between 15° and 40° at 45° incidence angle and a platform altitude of 14000 m.*

Besides geometric decorrelation concerns discussed above there is an additional term effecting differential interferometric phase measurements not considered for spaceborne applications. The repeat pass interferometric phase is given by

$$\phi \approx \frac{4\pi}{\lambda}\left(-\underbrace{\langle \hat{l}, \mathbf{b} \rangle}_{\text{topo term}} + \underbrace{\langle \hat{l}, \mathbf{D} \rangle}_{\text{disp term}} - \underbrace{\frac{1}{\rho}\langle \mathbf{D}, \mathbf{b} \rangle}_{\text{forgotten term}} \right) \tag{3}$$

where $\vec{D}$ is displacement of the surface between observations. Assuming the topographic term is eliminated using a DEM (such as from SRTM or single pass interferometry) or through techniques such a three pass or four pass interferometry then the differential interferometric phase is given by

$$\phi \approx \frac{4\pi}{\lambda}\left(\underbrace{\langle \hat{l}, \mathbf{D} \rangle}_{\text{disp term}} - \underbrace{\frac{1}{\rho}\langle \mathbf{D}, \mathbf{b} \rangle}_{\text{forgotten term}} \right) \tag{4}$$

The last term in Equation 4 can be safely ignored for most spaceborne applications, however for airborne applications it could be a limiting source of error of systematic deformation in the scene (excluding atmosphere) if the baseline is not sufficiently small. Note that the displacement vector appears in both term is Equation 4. Since only the first term is desired either the second term must be kept sufficiently small or a method for solving and eliminating this term must be employed. Using three differential passes having an appropriate geometry one can solve for and eliminate the second term. Alternatively, by constraining the baseline length to be sufficiently small depending on the desired deformation mapping accuracy the second term can be ignored. Writing Equation 4 as

$$\phi \approx \frac{4\pi}{\lambda}\left(\underbrace{\langle \hat{l}, \mathbf{b} \rangle}_{\text{disp term}} - \underbrace{\frac{1}{\rho}\langle \mathbf{D}, \mathbf{b} \rangle}_{\text{forgotten term}} \right) = \phi_{\text{d}} - \underbrace{\frac{4\pi}{\lambda}\frac{1}{\rho}\text{Db}\cos\beta}_{\phi_{\text{for}}} \tag{5}$$

where β is the angle between the displacement and baseline vectors then the following inequality for the baseline length results from requiring the displacement associated to the second term to be less than a threshold, $\Delta\rho_{thres}$.

$$\begin{aligned} \phi_{\text{for}} \le \phi_{\text{thres}} &= \frac{4\pi}{\lambda}\Delta\rho_{\text{thres}} \\ \text{Db}\cos\beta \le \text{Db} &\le \rho\Delta\rho_{\text{thres}} \end{aligned} \tag{6}$$

Figure 4 shows the displacement error as function of displacement magnitude and baseline length. Assuming geophysical signals of interest (e.g. earthquakes) have magnitudes up to about 2 m and a desired mapping accuracy of 1 mm indicates that it is necessary to use a baseline length less than about 10 m.

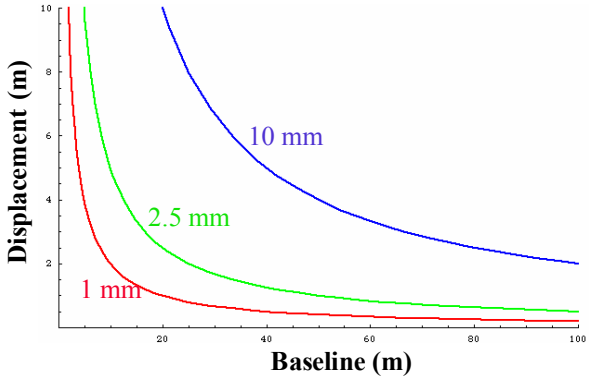

Figure 4. *Displacement error versus baseline length and displacement magnitude.*

Studies will determine the ability of each platform to fly within the required tube of 10 m (and desired tube of 1 m). We have conducted a study to assess the ability of a pilot to fly the Proteus aircraft (piloted) along desired flight tracks

with an on-course indication display in the cockpit that is described below. Our studies indicate that this is not a viable means of controlling the aircraft trajectory and modifications the Flight Management System (FMS), including modifications to support data ingestion of real-time GPS-determined state vectors into the FMS are key components of the required platform modifications.

C. The "Enhanced" Predator-B Aircraft: The ALTAIR

The ALTAIR is a derivative of the fully operational Predator UAV and is developed specifically for scientific and commercial applications that require large payload capacities with operations to 15,850 m (52,000 ft). The jet-powered turboprop ALTAIR can remain airborne for 32 hours. Equipped with fault-tolerant avionics, the ALTAIR is an extremely reliable and stable platform to meet a variety of mission scenarios. The ALTAIR is being developed at GA-ASI's flight operations facility in El Mirage, California adjacent to Edwards Air Force Base, under the supervision of NASA Dryden's ERAST UAV program. From the ALTAIR Experimenter's Handbook we found much of the information needed for initial design of a L-band radar.

The ALTAIR aircraft specifications are:

1) Wingspan: 26.2 m (86 ft)
2) Length: 11.0 m (36.2 ft)
3) Height: 3.6 m (11.8 ft)
4) Maximum payload: 300 kg (660 lb)
5) Maximum altitude: 15,850 m (52,000 ft)
6) Air speed: 60 – 200 knots
7) Endurance: 32 hours above 12,192 m
8) Maximum ferry range: 5170 nm
9) Power: 9 kW main, 4.5 kW backup (The UAV requires 2 kW)
10) Payload bay size: 46 ft^3
11) Safety: triple redundant control module, dual flight controls, dual electrical power systems, Traffic Avoidance and Collision Alert System (TCAS), ATC voice relay, mode 3C transponder, NASA approved flight termination system (FTS).
12) Navigation: remotely-piloted or fully-autonomous with three integrated INU and three Differential GPS units (optional P-code GPS)
13) Data link: C-band line-of-sight, Ku-band SATCOM over-the-horizon, or airborne relay.
14) Shipping size: fits inside a C-130 aircraft (64"W x 437" L x 78" H)
15) Payload bay is not pressurized.

D. The Proteus Aircraft

The Proteus aircraft is a very lightweight (6000 lb without payload and fuel) experimental aircraft that requires two pilots (or one pilot and a mission specialist) to operate. The aircraft could become a UAV if more funding is available for further development. Because it is a manned aircraft, the Proteus is certified by the FAA to take off and land at any airport equipped with a 6000-ft runway. However, it does require a large hangar for storage because the lightweight aircraft can be easily damaged by strong winds or heavy storms. The Proteus can fly in most weather conditions that a typical aircraft flies except for icing on the wings.

The Proteus aircraft is an unusual looking aircraft with a canard configuration and a pair of vertical tailplanes mounted on booms extending back from the rear wing (see Figure 2). The Proteus aircraft specifications are:

1) Aft wingspan: 23.6 m (77.6 ft)
2) Canard span: 16.7 m (54.7 ft)
3) Length: 17.2 m (56.3 ft)
4) Height: 5.4 m (17.6 ft)
5) Maximum payload: 900 kg
6) Maximum altitude: 18,593 m (61,000 ft)
7) Air speed: 220 knots at 13.7 km (45,000 ft)
8) Endurance: 8 to 10 hours (pilot restriction)
9) Maximum ferry range: > 2000 nmiles
10) Payload power: 11.2 kW (28 V-dc)
11) Payload size: limited by the pod size, which can be as big as 10 m x 1.2 m x 1.2 m
12) Navigation: Garmin GPS receiver and Boeing's GPS stabilized INU with a 1 Hz update rate (attitude is updated at 10 Hz).
13) SATCOM link: via INMARSAT (2400 baud); via Iridium (9600 baud).
14) Standard payload pod is not pressurized. Pressurized pod would double the pod cost.

E. Proteus Flight Path Stability

At a flying altitude of 13.7 km (45,000 ft), the Proteus aircraft is flown manually by the pilot. The ability to stay within a 5 – 10 m tube at this altitude is heavily dependent upon the accuracy of the real-time DGPS (which the Proteus currently does not have) and the skills of the pilot. We conducted an experiment in conjunction with Scaled Composites and NASA Dryden Research Center to assess the ability of a pilot to fly the Proteus within a 10 m tube [1]. We provide a brief description of the results below (a detailed description is in [1].

For the experiment we collected position data for three flight lines approximately 100 km length (with two of the flight lines orthogonal) at an flight altitude of 45000 ft (13716 m) to see how well the pilots can control the aircraft with varying wind conditions aloft. We modified the real-time GPS equipment developed at JPL and wrote a PC based

program to provide the pilot with real-time display of offsets from the desired trajectory. The system was installed on the Proteus aircraft along with a new antenna to receive the GPS correction data needed to get the submeter accuracy that is achieved by the system. We recorded the position data at a 1 Hz rate and obtained 10 Hz attitude angle data recorded by the Proteus telemetry system.

The experiment was flown on August 21, 2003 and all three lines were successfully collected and the data has been analyzed. Figure 5 shows the location of the three lines that were flown.

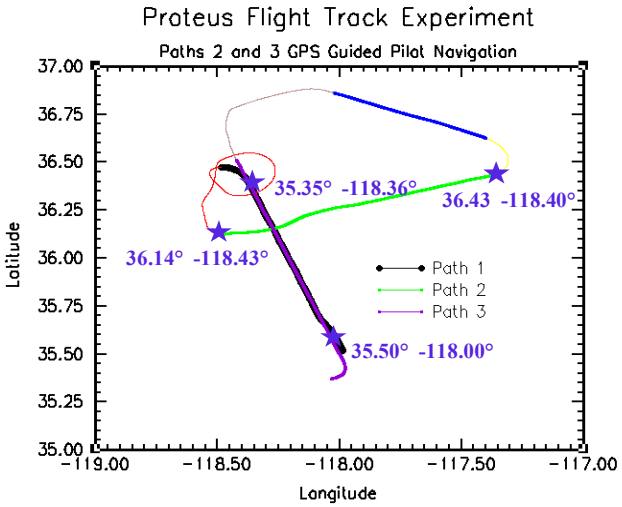

Figure 5. *Location of experimental flight lines of Proteus aircraft.*

The third pass was by far the best pass and was indicative of the pilots learning to fly the aircraft more effectively using the GPS navigation display. The pilots were much better able to maintain position within a 10 m tube, however most of the time the aircraft was outside the required 10 m tube and even was outside a 50 m tube for a large fraction of points. For the third flight line the mean and standard deviation of the error in the cross-track position was 0.9 m and 25.8 m and was 2.0 m and 6.7 m for the vertical position. Figure 6 shows the cross track and vertical offsets with a 10 m (small blue ellipse) and 50 m tube (large blue ellipse) overlain. Moreover, the pilots indicated that flying the lines using the display was very tiring and that a 3 hour flight was probably about the longest flight a pilot could fly the aircraft that way. Attitude angle variations during the flight lines were very large and would severely impact the ability to generate high quality repeat-pass interferometric measurements.

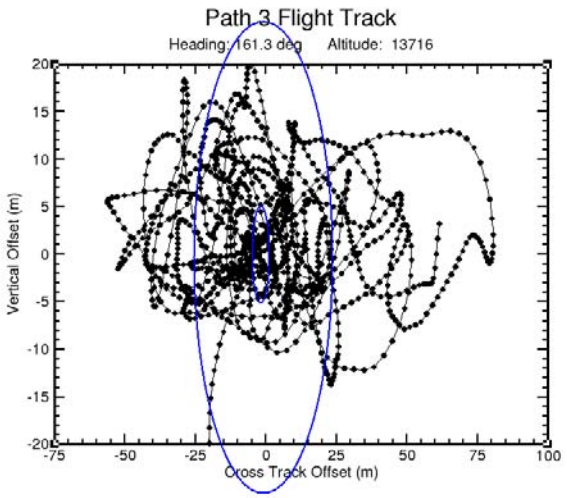

Figure 6. *Cross-track and vertical displacements for pilots manually controlling the Proteus aircraft to fly a desired trajectory.*

F. Proteus Antenna Location(s) and Baselines

The Proteus aircraft provides many options for mounting the L-band antenna(s). For a single-antenna system, the most obvious option is to mount the antenna on the side of the payload pod. This will minimize power loss and integration time. For an along-track interferometry system, it is possible to mount two L-band antennas at either end of the 10-m long payload pod to achieve a 7 m physical baseline. Alternatively, the fuselage of the aircraft could provide about a 10 m physical baseline. For single-pass cross-track interferometry, the two antennas could be mounted on either tailplanes on the aft-wings to provide a physical baseline of about 7 m.

G. Proteus Operational Scenario

The Proteus aircraft is operated by a pilot and a co-pilot who could provide minimal support to the payload, such as power cycling the instrument. Hence, radar operation has to be completely automated with self-diagnostic capabilities built into the system. A satellite link is available typically via INMARSAT with a low data rate of 2400 baud to provide limited communication with the radar instrument from the ground. On deployment, the Proteus aircraft crew consists of the two pilots and the crew chief (to service the aircraft). Permission to fly over air space is granted by the FAA similar to any manned aircraft, which is logistically easier than the Altair UAV and does not require the 60 day lead time allowing for rapid response to geophysical events of interest.

III. RADAR SYSTEM

The proposed radar for the UAV platform is a miniaturized polarimetric L-band radar for repeat-pass and single-pass interferometry with options for along-track interferometry and additional frequencies of operation. The radar will be appropriate for use both with existing radar testbed platforms as well as for installation on an UAV. Such a system will demonstrate key measurements both to NASA including:

- Precision topography change for monitoring earthquakes both during and after a seismic event,

for monitoring volcanic activity and for monitoring human-induced surface change such as subsidence induced by oil or water withdrawal, or other displacements of the surface from tunneling activities.

- ➢ Polarimetric interferometry, which can provide NASA with measurements of forest structure and sub-canopy topography.
- ➢ Polarimetric tomography, mapping in detail the vertical structure of a vegetated area.

The philosophy of the radar design is as follows: the design should be modular, compact, light-weight, and adaptable to the UAV and other airborne platforms. The design should also be flexible so that this radar platform may serve as a testbed to demonstrate new radar technology and techniques.

Repeat-pass interferometry (RPI) for surface deformation requires precise knowledge of motion and location, stability of the baseline to within a 5 – 10 m tube, and stability of the attitude in order to have Doppler centroids from two data passes to agree to a fraction of a beamwidth for adequate coherence. Precise knowledge of motion and location is provided by the high precision INU and real-time differential GPS receivers. Doppler centroid stability can be achieved by along track electronic beam-steering up to ±15º linked to the INU attitude angle measurements. This dictates the radar design to utilize an active array antenna with transmit/receive (T/R) modules and phase shifters with a beam steering angle resolution of better than 1°.

An important selection criterion for the platform is its suitability for hosting a L-band radar and possible future upgrades to the system. As this SAR will be operated on a UAV, there will be no radar operator. Based on a data file provided by flight planning software, the UAVSAR will automatically initiate data takes at the appropriate locations throughout the flight. This approach was implemented on GeoSAR (a radar interferometric mapping system designed and built by JPL and currently operated by Earthdata International which is hosted on a Gulfstream II aircraft) with good results. Because of the autonomous requirement, this instrument must include BIT (Built In Test) capability and be able to determine failure at the unit level. A modular approach to delineation of logic functions in the instrument will assist in the addition of potential options in the future. Because the instrument is designed for modularity, reconfiguration for the addition of potential options or installation on a different platform should be feasible. The goal is to be able to fly on either an ALTAIR or a Proteus aircraft.

Based on the Proteus and ALTAIR's altitude of 13.7 km (45,000 ft), we designed a fully polarimetric L-band radar with 80 MHz bandwidth and 16 km range swath. This radar has an active electronic beam steering antenna to achieve Doppler centroid stability that is necessary for repeat-pass interferometry.

In the following sections, we will outline the radar design for the L-band polarimetric RPI radar and its expected performance. We will also describe the hardware configuration and potential opportunities for technology demonstration. We will then discuss two add-on options: the L-band cross-track or along-track interferometer and a high frequency (C, X, or Ku)-band polarimetric and cross-track interferometric radar.

A. Instrument Overview

Based on the science objectives and UAV platform characteristics, the key parameters of the radar design include:

Frequency:	1.26 GHz (0.2379 m)
Bandwidth:	80 MHz
Pulse duration:	40 μsec
Polarization:	Fully polarimetric
Interferometry:	Repeat-Pass
Range swath:	16 km
Look angle:	30º - 60º
Transmitter:	2.0 kW peak power
Antenna size:	0.5 m x 1.6 m with electronic beam steering capability
PRF:	1600 Hz (interleaving H and V transmit polarizations)
Altitude:	13.7 km
Ground speed:	100 m/s

B. Hardware Configuration

The radar instrument is made up of three major subsystems: the RF electronics subsystem (RFES), the digital electronics subsystem (DES) and the antenna subsystem. Figure 7 is a simplified instrument block diagram of the L-band radar.

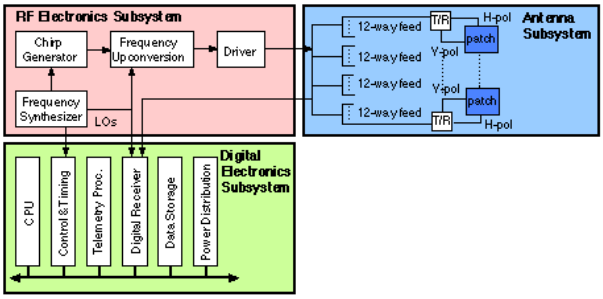

Figure 7. *Simplified instrument block diagram of the L-band Repeat-Pass Interferometer.*

The RFES performs the transmit chirp generation, frequency up-conversion, filtering, and amplification during signal transmission. The RFES also controls the routing of the radar signal and the calibration signal.

The DES performs overall control and timing for the radar, frequency down-converts and digitizes the received echo, and routes the data to on-board data storage. The dual-channel digital receiver employs two high-speed analog-to-digital converters (ADCs) capable of handling L-band signals to perform sub-harmonic sampling of the radar echoes. Filtering is performed by the digital filters implemented on field-programmable gate arrays (FPGAs). This approach saves cost, mass, and power while provides tremendous flexibility in the frequency selection of the digital filters. The sub-harmonic sampling technique is frequently used in the communication industry at lower frequencies. The recent availability of high-speed ADCs capable of handling L-band signals makes this technique feasible for radar applications, but has not yet been demonstrated with SAR systems.

The antenna subsystem performs beam steering, transmission, and high power amplification on transmit and low noise amplification on receive. The antenna is a dual-polarization corporate-fed planar phased-array with 4 x 12 T/R modules and phase shifters for electronic beam steering from radar pulse to pulse. The peak transmit power for each T/R module is 40 W and the combined power of the 48 T/R modules is approximately 2.0 kW. Typical efficiency for L-band solid state amplifiers (SSPAs) is 40 %. On the transmit end, there will be a polarization switch to direct the transmit signal to either the H or V-polarization feed of the antenna element. On the receive end, each T/R module will have two receiver front-ends (pre-select filter, high power limiter, and low-noise amplifier) to accommodate radar echoes from both the H and V-polarizations.

C. Estimate of Power, Weight, Volume

The estimated D.C. power for the L-band polarimetric RPI is just under 1 kW when the radar is transmitting. This is well within the capacity of the ALTAIR UAV or the Proteus aircraft. The standby D.C. power should be on the order of 150 W. The active array antenna should weigh less than 80 kg since each T/R module weighs about 0.5 kg. The remainder of the radar electronics in the payload bay should weigh less than 100 kg (approximately 20 kg for the RFES, 30 kg for the DES, and 30 kg for cabling, power distribution, etc.).

D. Radar Upgrade Options

We have assessed the possibility of adding L-band along-track or cross-track interferometry on both the Proteus and ALTAIR platforms. The performance and cost of the L-band interferometry options are heavily dependent on the placement of the second antenna on the aircraft. Other hardware changes for interferometry would be the addition of some extra switches in the switching network, and the necessary timing signals for controlling these switches. Further study is needed to determine these parameters.

E. L-band Cross-Track Interferometry Option

L-band cross-track interferometry may be achieved by placing two antennas at the hard points underneath the wings of the ALTAIR, which are 3.7 m apart. The expected height accuracy should be better than 3 m, which is a significant improvement from the AIRSAR's L-band interferometer height accuracy of 5 to 10 m. For the Proteus aircraft, the two antennas could be mounted on either tailplanes on the aft-wings to provide a physical baseline of about 7 m to achieve a height accuracy of about 1 m. Polarimetric XTI may be achieved if both the antennas are dual-polarized and H & V polarized pulses are transmitted in an interleaving manner.

F. L-band Along-Track Interferometry Option

L-band along-track interferometry may be achieved by placing two antennas at the front end and tail end of the platform respectively. For the ALTAIR, the maximum physical baseline is 3 to 4 m depending on the length of the antenna. This is significantly shorter than the AIRSAR's physical baseline of 20 m and is not likely to be a viable mode for this platform. For the Proteus aircraft, the physical baseline is 7 to 10 m depending on whether we mount the antenna pairs on the payload pod or the fuselage of the aircraft. This antenna separation is nearly optimal for L-band ATI given the platform speed of 100 m/s for the Proteus.

Addition of a second frequency radar would be more involved than the addition of an interferometric capability.

For the second frequency radar, it would be necessary to add: An additional Up-Converter unit, an additional Switching Network, an additional antenna panel, a pair of additional receivers for down-conversion and a pair of additional digital channels to the digital system. This option could be implemented in the Proteus aircraft without modifying the anticipated mechanical packaging approach. In order to implement this option in the Predator-B aircraft, it is quite possible that a more efficient mechanical packaging approach would need to be pursued.

G. High Frequency Cross-Track Interferometry Option

High frequency XTI and polarimatric capability are key components of the hydrology discipline, which could be used to measure snow wetness, river level changes, etc and cold land processes, which could be used for ice thickness and ice age determination. This capability would require a pair of antennas, a pair of receiver front-ends to down-convert the signal to an L-band signal, an additional pair of L-band digital receivers, an additional chirp generator card with frequency up-conversion to the desired frequency, and added on-board data storage.

ACKNOWLEDGMENTS

This paper was written at the Jet Propulsion Laboratory, California Institute of Technology, under contract with the National Aeronautics and Space Administration. We would like to thank John Sharkey and Randy Albertson at NASA Dryden Research Center for valuable discussions of UAV systems and their capabilities and the engineers at General Atomics and Scaled Composites for providing their time and information concerning the proposed platforms and their capabilities.

Reference herein to any specific commercial product, process, or service by trade name, trademark, manufacturer, or otherwise, does not constitute or imply its endorsement by the United States Government or the Jet Propulsion Laboratory, California Institute of Technology.

REFERENCES

[1] Muellerschoen, R. and Bar-Sever, Y., “Aviation Applications of NASA's Global Differential GPS System”, Proceedings of the 2nd AIAA "Unmanned Unlimited" Conf. and Workshop & Exhibit, AIAA Paper 2003-6618, Sept. 2003.